

Improving early strength and durability of eco-friendly mortars: Investigating the influence of limestone filler fineness and blast furnace slag combination

Ammar Noui^{1,a}, Ahmed Abderraouf Belkadi^{1,b}, Leila Zeghichi^{2,c}, Oussama Kessal^{1,d}, Mohammed Sallah Bouglada^{3,e}, Yacine Achour^{1,f}, João Castro Gomes^{4,g}

¹Department of Civil Engineering Faculty of Sciences and Technology University Mohamed El Bachir El Ibrahimy of Bordj Bou Arreridj ElAnasser 34030 Algeria

²Department of Civil Engineering and Hydraulic Mohamed Khider University Biskra Algeria

³Department of Civil Engineering Batna 2 University Algeria

⁴C-MADE Centre of Materials and Building Technologies Covilhã UBI University Portugal

Article Info

Abstract

Article history:

Received 07 Apr 2024

Accepted 01 July 2024

Keywords:

Blast furnace slag;

Limestone filler;

Ternary mortars;

Carbonation;

Chemical attack;

Durability

This study investigates eco-friendly approaches for enhancing the early mechanical strength and durability of mortars utilizing slag, a byproduct of the steel industry. Mortars incorporating slag often exhibit inferior strength and durability compared to those made with cement. The objective is to ameliorate these properties through the incorporation of limestone filler (LF) and granulated ground blast furnace slag (BFS) at varying proportions, either independently or in combination. The physical properties (gas permeability), mechanical properties (compressive and flexural strength at 2, 7, 28, 365, 1095 days), and durability (HCL chemical attack and carbonation) of the resultant mortars were assessed, along with their microstructure using scanning electron microscopy and mercury porosimeter. Experimental findings indicate that the inclusion of LF enhances the initial strength of ternary mortars containing 10-17.5% LF and 10-25% BFS, while subsequent hydration of BFS yields mortars with comparable or superior compressive strength and resistance to chemical attack (HCL) relative to the reference mortar after 365 days.

© 2024 MIM Research Group. All rights reserved.

1. Introduction

The chemical production process of Portland cement, which involves the use of clinker, accounts for 60-65% of CO₂ emissions during its manufacture [1,2]. Moreover, the clinkering process exerts a significant impact on natural sources of raw materials, which are depleting at an alarming rate [3]. Various strategies have been proposed to mitigate anthropogenic CO₂ emissions linked to clinker production by 5-8%. Among the technological solutions suggested, substituting clinker with industrial or natural waste shows promise in reducing total CO₂ emissions by approximately 37% [3,4].

Blast furnace slag (BFS) isn't just an add-on in concrete production; it's a sustainability champion. By incorporating BFS, concrete gains improved workability for easier placement, reduced heat of hydration to minimize cracking, enhanced long-term strength for lasting structures, and all while significantly lowering greenhouse gas emissions thanks to its partial replacement of clinker in cement [5-8]. However, a significant drawback of

*Corresponding author: ahmedabderraouf.belkadi@univ-bba.dz

^a orcid.org/0009-0005-6325-7131; ^b orcid.org/0009-0002-5978-9774; ^c orcid.org/0000-0003-2886-0339;

^d orcid.org/0000-0002-3669-6164; ^e orcid.org/0000-0001-9455-8686 ^f orcid.org/0000-0003-4249-5884;

^g orcid.org/0000-0002-2694-5462

DOI: <http://dx.doi.org/10.17515/resm2024.226ma0407rs>

Res. Eng. Struct. Mat. Vol. x Iss. x (xxxx) xx-xx

incorporating slag into Portland cement is its poor early-age strength, particularly evident at high replacement levels, attributed to the slow hydration kinetics of this cementitious additive [9-11]. To mitigate this limitation, numerous studies have been undertaken to expedite the hydration processes of slag within cementitious solutions [12,13]. Bougara et al. [12], suggest that the activation of hydration mechanisms at an early stage can be achieved through physical, thermal, or chemical means. Additionally, limestone filler (LF) has emerged as a recent addition to binary cementitious systems incorporating BFS [14,15]. Ternary mortars comprising LF and BFS demonstrate a superior cost-effectiveness ratio and reduced environmental footprint compared to slag-based materials [16], leading to enhanced hydration levels attributed to the dilution effect within the cement paste containing slag [17].

The primary drawback of incorporating slag into Portland cement is the poor early-age strength, especially noticeable at high replacement levels, owing to the slow development of hydration in this cementitious addition [9-11]. To mitigate this issue, various studies have endeavored to expedite the hydration reactions of slag within cement solutions. Bougara et al. [12] report that the activation of hydration processes at an early age can occur through physical, thermal, or chemical means, activation of hydration processes at an early age being physical, thermal or chemical [13]. The incorporation of limestone filler (LF) into binary blends containing blast furnace slag (BFS) is a recent innovation. This development has led to ternary mortars with LF and BFS boasting a more favorable cost-effectiveness ratio and a reduced environmental footprint compared to traditional slag-based materials [14,15] [16]. This leads to improved hydration levels due to the dilution effect in the cement paste containing slag [17] [18]. Berodier et al. [19] note that the rate of substitution and the fineness of the mineral addition introduced depend on this mechanism. Moreover, the presence of limestone in Portland cement leads to the formation of carboaluminate due to reactions between C_3A and $CaCO_3$. However, this production is limited to ages below 3 days because of the complete consumption of C_3A . In contrast, in ternary mortars containing limestone and a source of aluminosilicate, the aluminate-carbonate reaction persists at later ages. For instance, mixtures based on fly ash and limestone exhibit carboaluminates present up to 90 days [20,21], as do mixtures of metakaolin-limestone [22]. This results in an increase in compactness and mechanical strength due to the stabilization of ettringite, which causes an expansion in the volume of hydrates, thereby enhancing hydration levels [23,24] [17]. This study builds upon prior research investigating the properties of ternary composites combining ordinary Portland cement (OPC), LF, BFS. Previous studies have shown that these composites offer promising benefits. Gao et al. [25] found that incorporating 10% LF enhances the early-age compressive strength of BFS concrete while reducing CO_2 emissions and production costs. Similarly, Carraco et al. [26] demonstrated that, within the LF-BFS-OPC ternary mixture, LF and BFS contribute to increased early and later compressive strength, respectively.

Building on this concept, Menéndez et al. [27] developed a model to identify the ideal ternary mix for maximum strength and minimal porosity. Their model predicted a mortar containing 10% limestone and 10% slag for peak early-age compressive strength. Conversely, for later stages, the optimal mix shifted to an Ordinary Portland Cement (OPC) blend with 35% Blast Furnace Slag (BFS) and 7.5% Limestone Filler (LF) to achieve superior physical and mechanical properties. Deboucha et al. [9] studied how limestone and slag influence the chemical reactions in which water is absorbed by ternary cements. Their findings revealed that the degree of hydration is dependent on both the replacement level of these additives and the water-to-binder ratio employed.

Yu et al. [28] suggested that LF and BFS have the potential to enhance cement hydration and homogenize mixtures, thereby reducing pores, particularly in regions near aggregates

due to their filling effect and nucleation sites. when used in fabricating ternary composites. Xuan et al. [29] found that limestone filler (LF) and slag (BFS) work together to enhance a certain process (synergistic effect). while Adu-Amankwah et al. [17] noted that these same ternary blends (OPC-LF-BFS) have a low aluminum to silicon ratio (Al/Si). Arora et al. [30] established a linear function correlating monocarbonate formation with carbonate consumption.

Line with previous research. Bouaskeret et al. [14] reported that incorporating limestone filler (LF) between 10% and 20% effectively hinders the development of endogenous shrinkage and prevents initial cracking in cement-blast furnace slag (BFS) systems. Similarly. Itimet et al. [31] they discovered that adding up to 15% limestone filler (LF) with the right amount of slag (BFS) can lessen the concrete's shrinkage caused by water loss. Investigating the impact of limestone fineness. Briki et al. [32] found that replacing 20% of clinker with finer limestone (BSS = 4.21 m²/g) resulted in comparable strength to OPC up to 7 days. This improvement is attributed to enhanced cement hydration. which compensates for the dilution effect of limestone.

However. despite these prior studies. there remains a significant gap in research regarding ternary mortars. For instance. microscopic analyses to comprehend macroscopic phenomena must be undertaken. Therefore. an exhaustive investigation was imperative to elucidate the impacts of dilution and nucleation in ternary mixtures (OPC-LF-BFS). Additionally. the effects of Blaine specific surface area (BSS) of slag and limestone on ternary composites have not been thoroughly explored based on previous research. According to the authors of this study. no research was found on the long-term mechanical behavior (365 and 1095 days) of ternary mortars (OPC-LF-BFS). Consequently. the durability of ternary cement-limestone-slag mortars has seldom been examined.

To address these existing research gaps. this study scrutinizes the microstructural. mechanical properties. and durability of OPC-LF-BFS ternary mortars. Various experimental tests were conducted to evaluate compression and bending resistance (at ages of 2. 7. 28. 365. and 1095 days). employing scanning electron microscopy (SEM). mercury porosimetry (MIP). gauze permeability. carbonation. and chemical attack (HCl).

The principal findings of this study are as follows: firstly. the properties of the ternary mixture were analyzed using both macroscopic and microscopic tests. Secondly. the experimental results delineated the effects of limestone and slag fineness and substitution rate. Thirdly. the durability of OPC-LF-BFS ternary mortars was assessed through immersion in 1.5% HCl solution. carbonation testing. and gauze permeability analysis.

2. Materials and Methods

2.1. Materials

In experimental tests. Portland clinker sourced from the Ain-El-Kébira cement plant (Sétif-Algeria) was ground to a fineness of 350 m²/kg. Gypsum. obtained from natural rock quarries near the same cement plant. with a 3% content rate. was utilized. with a hydrated calcium sulphate (CaSO₄•2H₂O) level of 76.4%. Granulated blast furnace slag (BFS) from El HADJAR. consisting of spherical grains with a particle size class of 0/5 mm. and limestone fillers (LF) from limestone rock deposits. were also ground to various Blaine-specific surface areas (BSS). The particle size distributions of the raw materials are depicted in Fig. 1. illustrating that limestone and slag contained a higher volume of fine particles compared to clinker.

Chemical compositions. determined by X-ray fluorescence (XRF) analysis. and physical properties (Blaine-specific surface and density) of OPC. LF. and BFS are presented in Tables 1 and 2. respectively.

Table 1. Chemical compositions of all powders used (wt. %)

	Clinker	Gypsum	Slag	Limestone filler
CaO	63.73	22.5	43.2	45.85
SiO ₂	21.42	3.8	41.1	12.74
Al ₂ O ₃	4.58	0.5	7	1.65
Fe ₂ O ₃	4.96	0.1	2.8	0.58
MgO	1.43	0.58	4.7	0.73
Na ₂ O	0.24	-	0.6	-
K ₂ O	0.32	-	0.32	0.24
SO ₃	0.72	32.84	0.25	0.11
L.O.I	2.62	39.09	-	37.54

Table 2. The Blaine specific surface area (BSS) and density of all powders.

	Clinker	Gypsum	Slag	Limestone filler
BSS1 (m ² /kg)	350	350	350	350
BSS2(m ² /kg)	-	-	550	550
Absolute density (kg/m ³)	3200	2340	2800	2600
Apparent density(kg/m ³)	1300	980	1000	1030

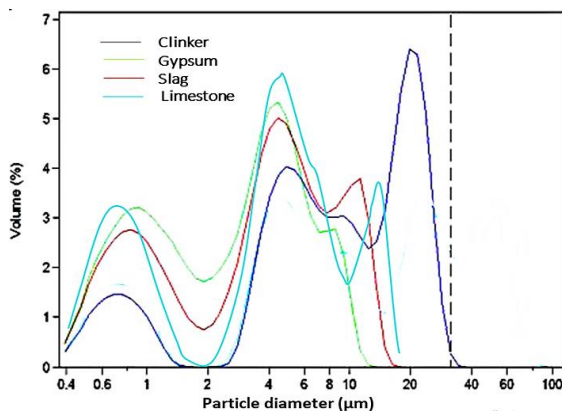


Fig. 1. Particle size analysis of clinker, slag and limestone

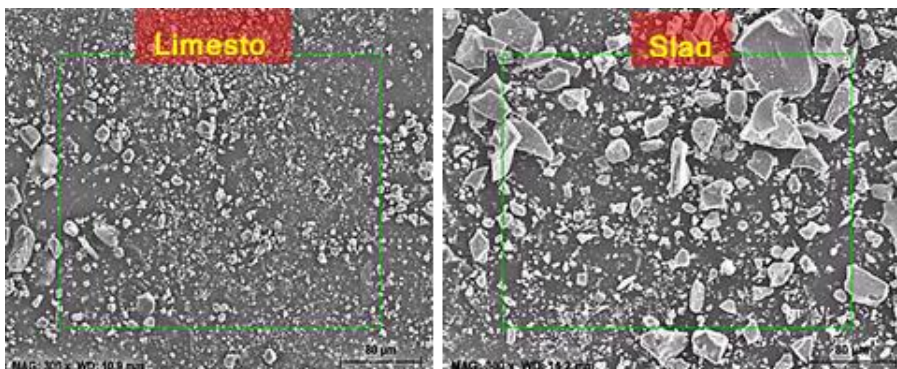


Fig. 2. SEM images of the raw materials

Additionally, standardized siliceous sand (0/3), meeting EN196-1 [33] standards, was employed. Fig. 2 showcases the particle morphologies of blast furnace slag and limestone filler powders. Coarse BFS particles larger than 10 μm exhibit a crushed gravel appearance with a uniform shape, a highly compact morphological structure, and a smooth surface.

2.2. Preparation of Mixtures

This study adhered to EN 196-1 standard [33] for mortar preparation, incorporating limestone filler (LF) and granulated blast furnace slag (BFS) as partial cement replacements (up to 35% by weight) in various combinations with differing fineness (refer to Table 3). A fixed water-to-binder ratio of 0.50 and sand-to-cement ratio of 3:1 were maintained for all mixtures. After casting in molds for 24 hours, the mortars were cured by immersion in water at a controlled temperature (23°C ± 2°C). The specific composition details for each mixture are provided in Table 3.

Table 3. Mixtures proportions

	Mixture (ID) Labels	Clinker (%)	Gypsum (%)	BFS (%)	LF (%)	W/L
1	0S-0L	97	3	-	0.5	0.5
2	3S-0L	62	3	-	0.5	0.5
3	0S-35L	62	3	35	0.5	0.5
4	10S1-25L1	62	3	10	25	0.5
5	10S2-25L1	62	3	10	25	0.5
6	10S1-25L2	62	3	10	25	0.5
7	10S2-25L2	62	3	10	25	0.5
8	17S1-17L1	62	3	17.5	17.5	0.5
9	17S1-17L2	62	3	17.5	17.5	0.5
10	17S2-17L1	62	3	17.5	17.5	0.5
11	17S2-17L2	62	3	17.5	17.5	0.5
12	25S1-10L1	62	3	10	25	0.5
13	25S1-10L2	62	3	10	25	0.5
14	25S2-10L1	62	3	10	25	0.5
15	25S2-10L2	62	3	10	25	0.5

2.3. Experimental Tests

Table 4 shows the experimental tests used in this study, their fields of application and measurement times.

Table 4. Experimental methods and fields of applications

Method	Test sample	Test time
Compressive strength	All samples (Mixtures from 1 to 15)	2, 7, 28, 365 and 1095 days
Flexural strength	All samples (Mixtures from 1 to 15)	2, 7, 28, 365 and 1095 days
Permeability	Mixtures (Mixtures 1, 2, 3 and 8)	28 Days
Carbonation	Mixtures (Mixtures 1, 2, 3 and 8)	28 Days+15 Days (in the carbonation chamber)
SEM	Mixtures (5, 9, 11, 13 and 14)	365 Days
MIP	Mixtures (1, 2, 3, 5, 9, 11, 13 and 14)	365 Days
Chemical attacks (1.5 % HCL)	All samples (Mixtures from 1 to 15)	200 Days

2.3.1. Compressive and Flexural Strength

The compression and flexural strength tests were conducted using an apparatus with a maximum capacity of 3000 KN. These mechanical properties were determined in accordance with standard [33]. The molds used had dimensions of 40 × 40 × 160 mm. Four samples of each mixture were tested at 2. 7. 28. 365. and 1095 days after casting. The average strength value was used to represent the ultimate flexural and compressive strength for each mixture.

2.3.2. Scanning Electron Microscope (SEM)

To better understand the macrostructural phenomena, a microstructural analysis of various mixtures was performed after 365 days using a Hitachi S-3400N scanning electron microscope (SEM).

2.3.3. Mercury Porosimeter

Mercury intrusion porosimeter (MIP) is a technique employed in this study to analyze the pore size distribution within the mortar samples [34,35]. An Autopore IV-Micromeritics mercury porosimeter was used, capable of applying high pressures (up to 414 MPa) to force mercury into pores as small as 3.6 nanometers and as large as 360 micrometers. By analyzing the pressure required for mercury intrusion, researchers can determine the distribution of pore sizes within the mortars.

2.3.4. Oxygen Permeability

The O₂ oxygen permeability method, which evaluates gas penetration resistance and transfer properties in cementitious mortars, was employed. After drying in a 105°C oven until constant weight was achieved (48 hours), 11 cm diameter and 5 cm thick specimens were laterally sealed and vertically confined to ensure unidirectional radial oxygen flow. Intrinsic permeability (K_{int}) was then calculated from apparent permeability (K_a) measurements at three absolute pressures (2, 3, and 4 bar) using the inverse of the average pressure (refer to equation 1 for details).

$$K_a = 2Q * P_{atm} * L * \frac{\mu}{P_2 - P_{atm2}} * A \quad (1)$$

Where Q is the volume flow at the inlet (cm³/s), μ is the dynamic viscosity of oxygen at 20°C±2°C equal to 2.0210–5 Pa. P is the absolute pressure at l input (bar), P_{atm} is the atmospheric pressure (bar), L is the thickness of the sample (m) and A the section (m²).

The Klinkenberg approach [36] was employed to isolate the intrinsic permeability, representing only the viscous flow of the permeating fluid. This value is determined through linear regression of various apparent permeability values in relation to the inverse of the average pressure (calculated as the mean between atmospheric pressure and gas inlet pressure) [37] [38]. It is defined as follows:

$$K = K_{int} \left(1 + \frac{\beta}{P_{moy}} \right) \quad (2)$$

$$P_{moy} = (P_0 + P_{atm})/2 \quad (3)$$

With β : the Klinkenberg coefficient, P_0 : atmospheric pressure and β . K_{int} is the slope of the Klinkenberg line.

2.3.5. Accelerated Carbonation

To assess CO₂ penetration resistance, an accelerated carbonation test based on the NF P18-458 458 standard [39] was conducted. After 28 days of water curing, cylindrical mortar

specimens (110 x 220 mm) were sectioned into four discs (approximately 5 cm thick). To ensure unidirectional carbonation, all sides except the sawn face were sealed with self-adhesive aluminum foil. Following a 14-day drying period at 60°C, one quarter of the specimens were placed in a dedicated chamber maintained at 4% CO₂, 65% ± 5% relative humidity, and 20°C for a month.

2.3.6. Chemical Attack

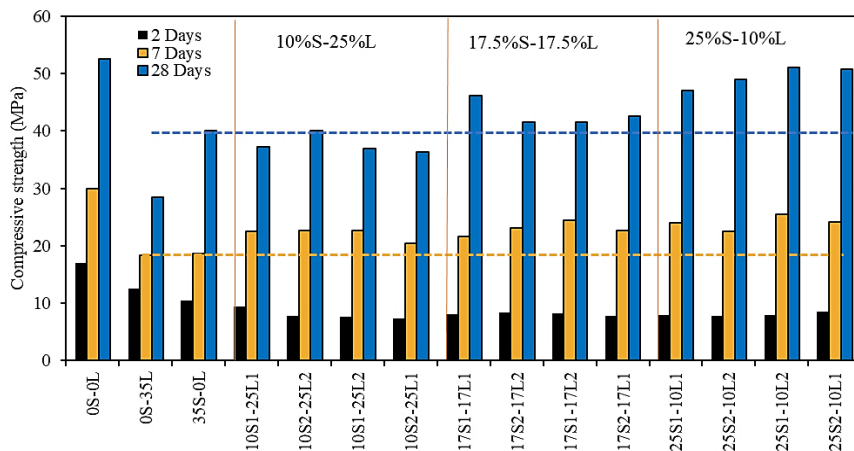
Following 24 hours in molds, mortar samples were cured in water for 28 days. They were then conditioned in a controlled environment (50% relative humidity, 20°C) until reaching constant weight before immersion in a 1.5% hydrochloric acid (HCl) solution for 200 days. This process simulates chemical attack, and the samples were subsequently evaluated for physical and mechanical properties to assess their durability.

3. Results and Discussion

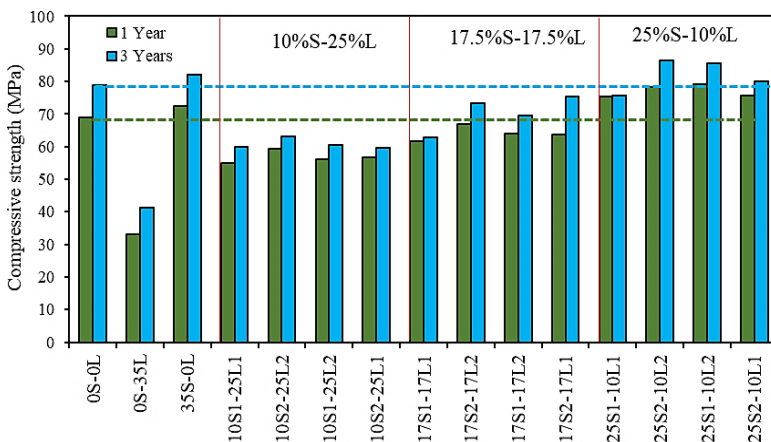
3.1. Compressive Strength

The results of the evolution of the compressive strength of mortars formulated with slag and limestone in the short and long term were presented in Fig. 3a and 3b, respectively. At the two-day mark, the 0S-0L blend exhibited superior compressive strength compared to other mixtures. This can be attributed primarily to the dilution effect caused by the inclusion of limestone filler and slag [7,40]. Consequently, the compressive strength of 0S-35L exceeded that of 35S-0L by 19%, attributed to LF acting as nucleation sites, facilitating additional C-S-H formation and enhancing cement hydration kinetics [5,41]. Moreover, LF was noted to fill voids, increasing mixture compactness and altering reaction rates at early stages [42]. However, the combination and fineness of LF and BFS had minimal effect on compressive strength at this early stage.

Thermogravimetric analysis revealed that calcite consumption increased over time, particularly after 28 and 90 days, indicating slower calcite reaction kinetics with aluminates from slag to form hemi/monocarboaluminates [9] [30]. Although comparable compressive strengths were observed for 35S-0L and 0S-35L after 7 days, a remarkable increase in strength was noted in blends containing LF and BFS additions. For instance, mortars like 10S1-25L1, 17S1-17L1, 17S1-17L2, and 25S1-10L2 exhibited substantial increases in strength compared to 35S-0L and 0S-35L [30].



(a)



(b)

Fig. 3. The compressive strength of various mixtures in (a) the short-term and (b) long-term

This increase was attributed to the formation of hemi/monocarboaluminate, preventing ettringite transformation into monosulphate and resulting in higher total hydrate volume and hydration reaction rates [21]. However, the compressive strength of mortar with these additions was slightly lower compared to the control (0S-0L), indicating that while hemi/monocarboaluminate formation offset the dilution effect, it couldn't fully compensate for the decline in cement hydrates[43]. Additionally, LF with a higher specific surface caused higher resistance, and finely ground limestone was found to improve hydration and compensate for dilution caused by clinker reduction [32].

After 28 days, while the compressive strength of 35S-0L was significantly higher than that of 0S-35L, it remained lower than that of 0S-0L by 30.9%. Ternary blends with high slag content showed notable strength increases over 35S-0L and 0S-35L due to various factors such as nucleation of C-S-H, ettringite stabilization, and carboaluminate formation. However, the presence of LF with a high-rate induced performance decreases due to dilution. Compared to 35S-0L, certain composites like 25S1-10L1, 25S2-10L2, 25S1-10L2, and 25S2-10L1 showed increased strength, while slight decreases were observed compared to 0S-0L. Moreover, the higher fineness of additions, particularly LF, led to better performance, contributing to capillary pore filling and mortar property improvement. While ternary mixtures with low BFS content showed lower resistance compared to 0S-0L and other ternary composites after one and three years, 35S-0L exhibited higher strength compared to 0S-0L controls. Overall, the study highlights the importance of material fineness in short and long-term reactions, emphasizing the necessity of alumina sources for carboaluminates formation and the optimal LF content for improved mortar strength. Furthermore, an increase of 14% in compressive strength at the one-year mark was observed with the addition of 25% BFS and 10% LF to cementitious mortars. This underscores the significance of maintaining carboaluminate formation for extended periods, as observed in mixtures containing limestone and aluminosilicate sources [42]. The presence of AFm phases was linked to calcite and reactive aluminates from limestone and slag, potentially explaining the lower long-term resistance of certain mixtures [44]. Studies suggest that using an ideal limestone content ensures the utilization of all active alumina from pozzolans in ternary binders [45]. In this study, 10% LF was

deemed optimal, highlighting the importance of balanced material compositions for optimal mortar performance.

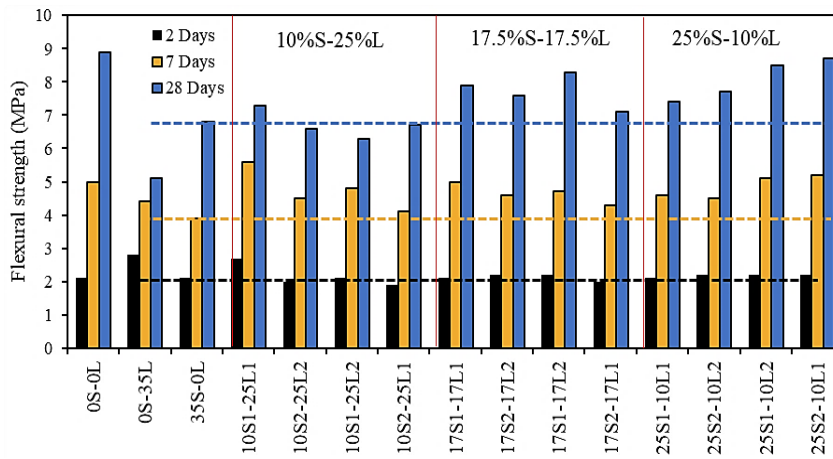
In summary, the fineness of materials significantly influences the reactions in ternary mixtures in both short and long terms, particularly for limestone fillers. Maintaining the formation of carboaluminates for up to three years requires adequate alumina sources in the ternary mixtures. Adding 25% slag (BFS) and 10% limestone filler (LF) boosted the mortar's compressive strength by 14% after one year. This highlights the importance of precisely formulated compositions for achieving superior mortar performance.

3.2. Flexural Strength

The flexural strength of mortars containing various additions at different ages (2, 7, 28, 365, and 1095 days) is illustrated in Figure 4(a) and (b). Similar to the compressive strength trend, flexural strength development varied across ages for different mixtures.

- At early ages (2 days), 0S-35L containing LF exhibited the highest flexural strength, likely due to improved packing and reduced capillary porosity [41].
- By 7 days, ternary blends showed similar flexural strength to the control mortar (0S-0L) and surpassed the strength of 35S-0L (BFS only). The enhanced strength is ascribed to the combined effects of limestone filler (LF) promoting nucleation and the early formation of Hemicarboaluminates (HC), which contribute to a stronger structure.
- Interestingly, long-term (1 and 3 years) results showed a greater increase in flexural strength compared to compressive strength for ternary blends with a low LF content (25% BFS, 10% LF). This suggests that carboaluminates formed in these mixtures are more effective in improving flexural strength than compressive strength [46]. This translates to stronger and more robust carboaluminate particles that contribute significantly to the enhanced mechanical performance of these eco-friendly mortars.

Overall, the flexural strength results support the findings from compressive strength analysis, highlighting the benefits of incorporating both BFS and LF in cementitious mortars, particularly at a 25% BFS and 10% LF ratio. The improved packing by LF and the formation of carboaluminates play a crucial role in strengthening these mortars over time.



(a)

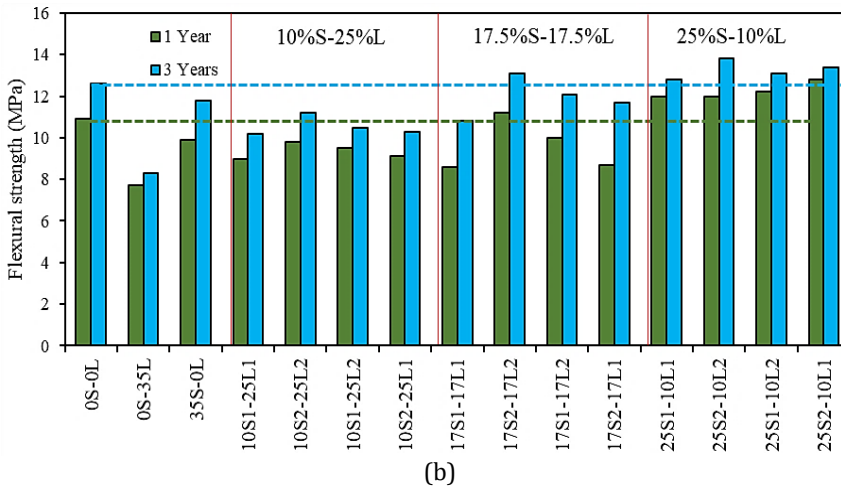


Fig. 4. Flexural strength of different mixtures in (a) the short-term and (b) long-term

3.3. Compressive vs. Flexural Strength Correlation

Figure 5 examines how well a mortar's compressive strength (resistance to crushing) translates to its flexural strength (resistance to bending) across the different mixture combinations. The results show a strong positive correlation ($R^2 = 0.97$), indicating that compressive strength generally increases along with flexural strength. Interestingly, the data points for early ages (2 and 7 days) are tightly clustered, while those for later ages (28 days, 1 year, and 3 years) are more dispersed.

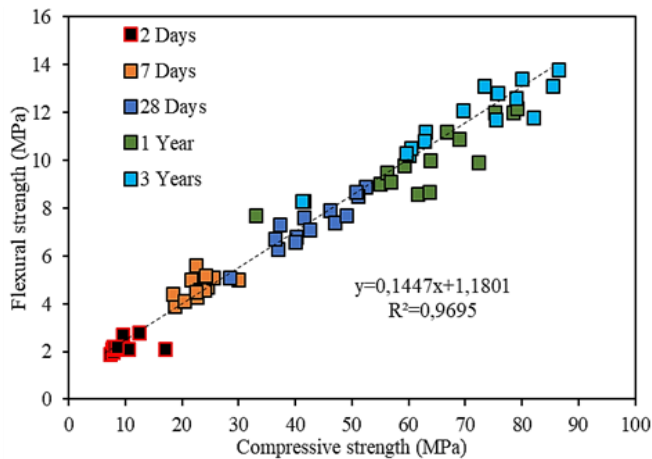


Fig. 5. Relationship between compressive and flexural strength

This suggests that at early ages, the variations in compressive and flexural strength between mixtures are relatively small. However, as the mixtures age and the effects of their composition and fineness become more pronounced, the mechanical properties diverge, leading to a wider spread of data points in the long term.

3.4. Mercury Porosity

To better understand the mechanical behavior of the different mortars studied, the pore size distribution was evaluated using a mercury porosimeter. Fig. 6 shows the results

obtained at 365 days. It can be seen that the 0S-0L mixture has a large number of pores with dimensions ranging between 0.02-0.4 μm . Additionally, for the same mixture, there is a wide distribution of pores between 0.2 and 2 μm , which corresponds to a high number of capillary pores. The 0S-35L mortar presents peaks between the ranges of 0.02-0.1 μm and 0.2-2 μm , indicating a considerable number of pores with these diameters.

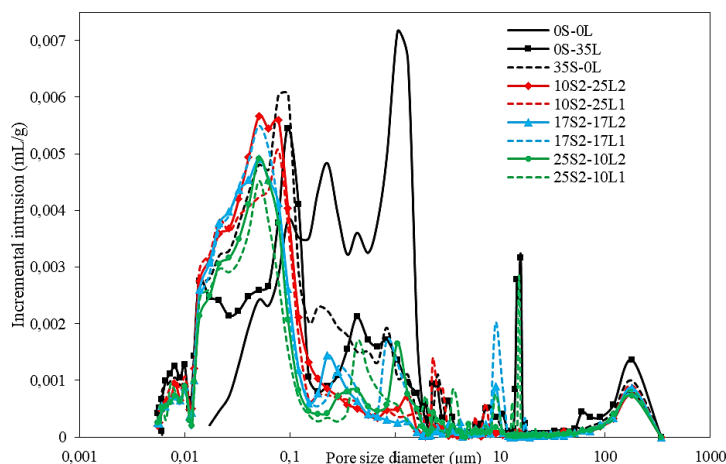


Fig. 6. Pore size variation in different mortars after one year

However, the 35S-0L binary composite shows fine pores varying between 0.01 μm and 0.1 μm , which is a result of the pozzolanic reaction of long-term slag producing a large volume of C-S-H that fills voids and capillary pores [47]. Additionally, the pore distribution of all mortars based on ternary types of cement is better compared to those based on binary binders or cement alone, as they evolve significantly towards fine pores. For example, the composites 25S2-10L1 and 25S2-10L2 reveal peaks between 0.01 and 0.03 μm with a total mercury intrusion of around 0.045 ml/g, indicating good compactness and homogeneity of these mixtures. Moreover, the decrease in pore size in the ternary mortars 25S2-10L1, 25S2-10L2 and 17S2-17L2 results in high mechanical performances (see Fig. 3). This is due to the phenomena of nucleation of C-S-H on CaO surfaces, the stabilization of ettringite, and the formation of carboaluminates of the clinker phase the ternary composite. These results were confirmed by Hadj Sadok et al. [7,48], which showed at 90 days a finer pore size distribution for mixtures containing slag and calcined sediment (15 %).

3.5. Accelerated Carbonation and Gas Permeability

The physical and chemical characteristics of building materials significantly influence their durability. Figure 7 explores how these properties affect transport phenomena, specifically focusing on accelerated carbonation and gas permeability, for the different mortar mixtures at 28 days of age. Figure 7 explores the relationship between material properties and transport phenomena (permeability and carbonation) for the different mortar mixtures at 28 days.

- Permeability:** The binary mixture with 35% LF (0S-35L) exhibited the lowest gas permeability ($1.01 \times 10^{-17} \text{ m}^2$) compared to other mixtures. This aligns with findings by Tsivilis et al. [49] and Panesar et al. [50] who attributed reduced permeability to LF's pore-filling effect. Conversely, the 35S-0L mortar (high BFS) showed higher permeability due to the slow hydration of BFS at early ages, creating more pores [9,11,51]. Interestingly, the ternary blend (17S1-17L1) demonstrated a significant permeability reduction compared to 35S-0L. Suggesting a beneficial interaction

between LF and BFS. This improvement in pore structure is likely due to the combined effects of pore filling by LF and nucleation sites provided by both BFS and LF. as suggested by Yu et al. [28] and Xuan et al. [29].

- **Carbonation:** The 0S-35L mortar displayed the lowest carbonation depth (0.25 cm). likely due to its denser microstructure achieved through LF addition. Conversely. the 35S-0L blend showed higher carbonation depths. which aligns with findings by Gruyaert et al. [52] due to its higher porosity. The mixture combining limestone filler and slag (17S1-17L1) resisted carbonation better than the one without (35S-0L). This improvement may be due to the formation of particles within the mixture (carboaluminates) that fill in tiny gaps and make the structure denser.
- The limited number of mixtures tested (four) due to travel constraints restricts broader conclusions. Further research is recommended to investigate the impact of varying BFS and LF contents and fineness on permeability and carbonation in ternary mixtures at later ages.

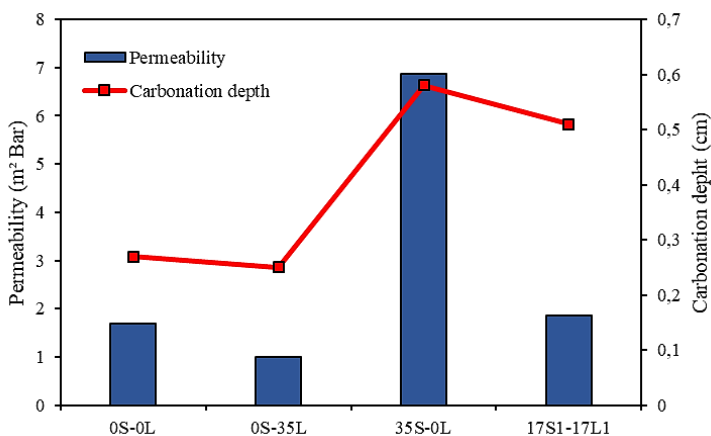
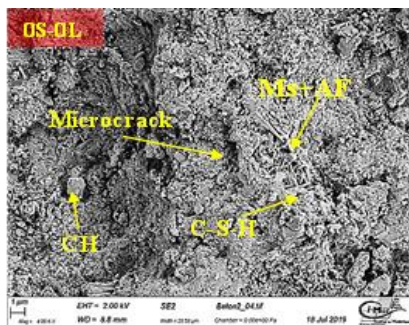
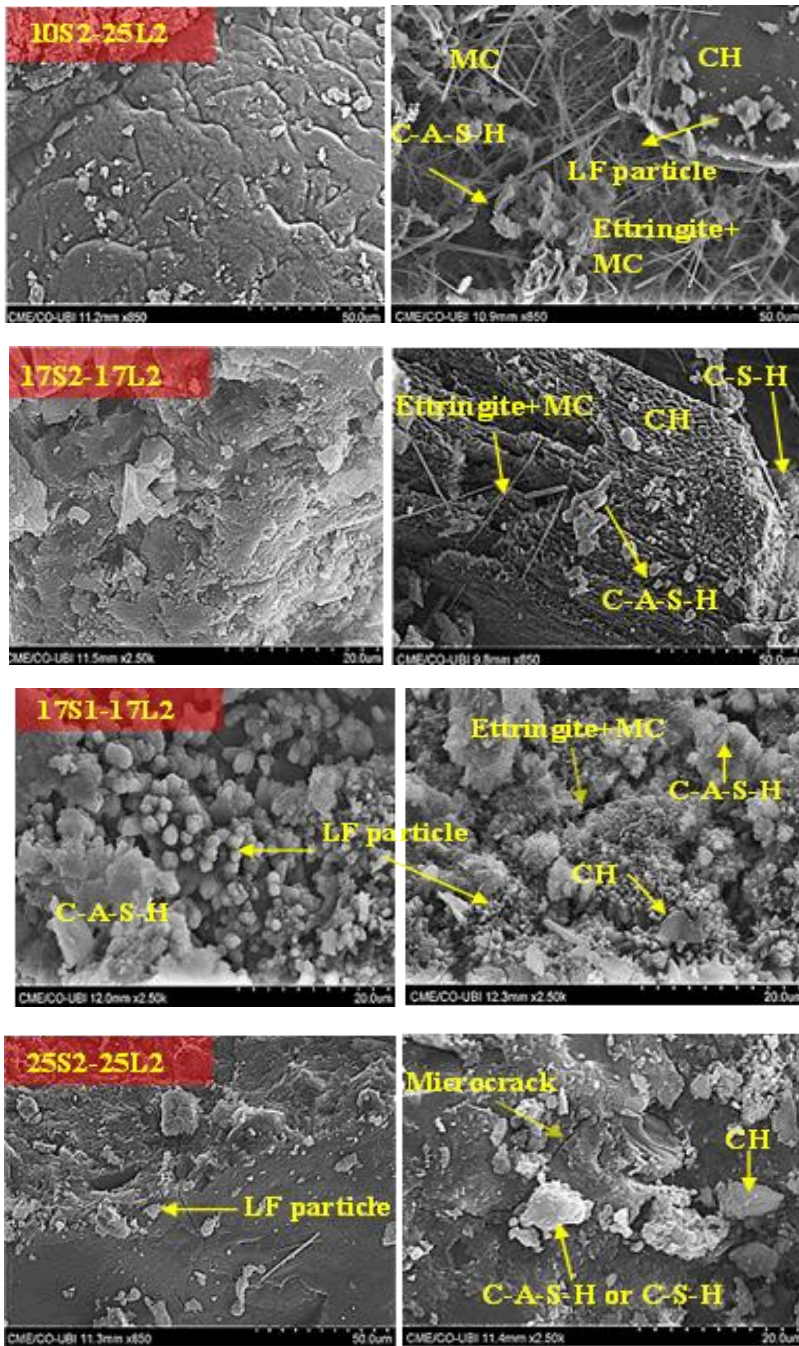


Fig. 7. Permeability and depth of carbonation of different mortars at 28 days

3.6. Scanned Electron Microscope (SEM)

The fig. 8 shows the results of the morphological analysis of hydrates after 365 days. The control paste's portlandite formed into a dense hexagonal crystal [53]. The hydration products, appearing as needles and flakes, were identified as AFt and Ms, respectively. Additionally, some capillary pores were discernible in the control mixture (0S-0L). These findings align with the results from the mercury porosimeter test in section 3.4. Conversely, the ternary mortars mainly exhibit the initial hydration phase.





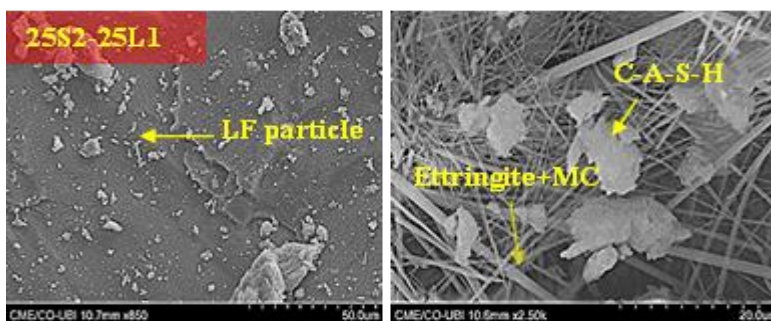


Fig. 8. The microstructures of various types of mortars

Despite the low clinker content in the ternary mixture, there are more hydrates present (C-(A)-S-H gel). It is also noted that Ms manifests as plates in the mixture without additives (0S-0L), while the introduction of LF and BFS alters these particles into Hc and Mc. The presence of C-A-S-H in the capillary pores significantly impacts transfer properties. Crystalline phases such as CO-AFm in needle-shaped form [54] (observed in mixture 25S2-25L1) effectively occupy capillary voids. The C-A-S-H resulting from the pozzolanic reaction can also play a significant role in masking the limestone dilution effect. The mortar 25S2-25L1 exhibits the highest compactness, correlating with the highest compressive strength. However, microcracks were observed on samples 25S2-25L2. According to Khalifa et al. [55], the high substitution rate and fineness of slag induce some microcracks due to the accelerated hydration rate of the composite.

3.7. Hydrochloric Acid Attack

In Fig. 9a and b, it can be observed that the loss of compressive strength and mass after 200 days of various mortars immersed in aggressive media (HCL (1.5 %)) is shown. The behavior of all mortars varies according to the nature of the aggressive medium. Concerning hydrochloric acid resistance, a significant 78% decrease in compressive strength is observed after 200 days of HCl exposure in the 35S1-0L1 composite [56]. This reduced resistance is attributed to the presence of a high number of pores at the age of 28 days, resulting in lower resistance to ionic penetration and compromising the stability of hydrated phases. Additionally, significant strength decreases of 75% and 68% are also observed in mortars 0S-0L and 0S1-35L1, respectively [57]. This is believed to be due to the sufficient amount of portlandite present in the OPC and LF, leading to the formation of gypsum, which is known to be expansive. Mass loss corroborates the compressive strength results. However, all ternary mortars exhibit a notable improvement in resistance against hydrochloric acid (HCl) attack compared to 35S1-0L and OPC. Mixtures 10S2-25L2, 17S1-17L1, and 25S1-10L2 show respective strength decreases of 50%, 42%, and 46% after 200 days in HCl, resulting in an approximately 85% increase in resistance to HCl attack for ternary mixtures.

The addition of pozzolanic materials with limestone is identified as a potential solution to improve sulfate resistance, as observed by Boubekour et al. Furthermore, the effect of fineness is noted, with higher Blaine specific surface (BSS) area resulting in a slight improvement in HCl resistance. Mixtures 10S2-25L2 and 25S2-10L2 show strength increases of 14% and 17% over 10S1-25L1 and 25S1-10L1, respectively. This is attributed to the accelerated hydration process, leading to a denser and more compact porous structure, as noted by Sia et al. Microstructural analysis reveals that the Si/Al-rich residues generated at the surface by the pozzolanic behavior of BFS effectively inhibit corrosion by acting as a barrier to chemical attack [58] [59].

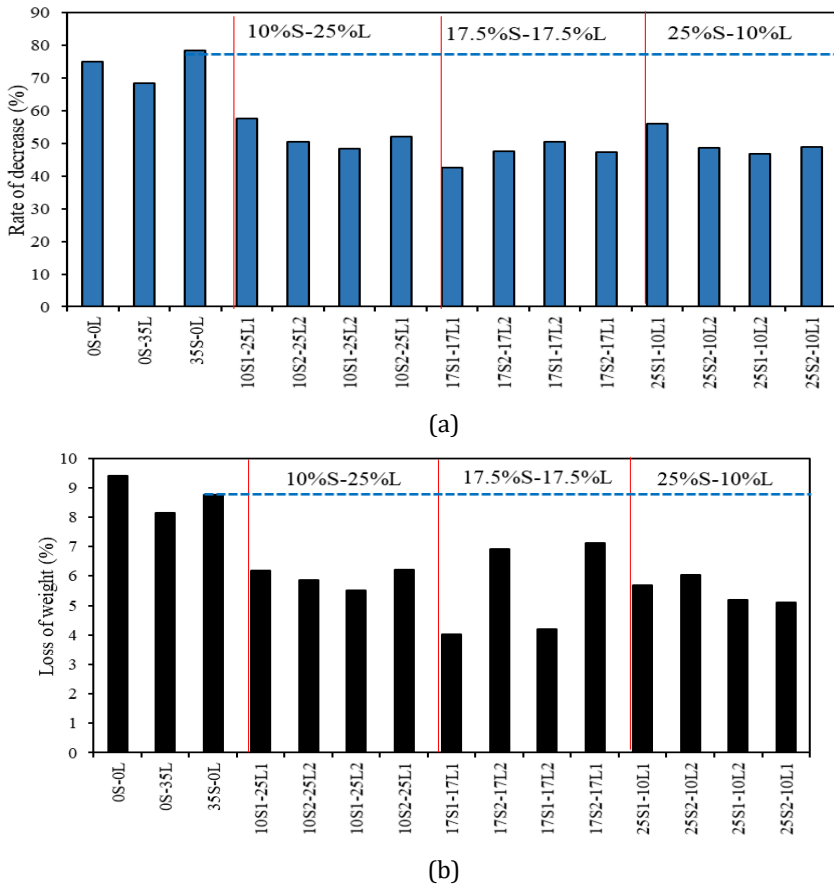


Fig. 9. Illustrates the percentage decrease in both compressive strength (a) and weight loss (b) for different mortar specimens

5. Environmental Assessment

The environmental analysis of the materials used in this study focuses on the energy consumption during the grinding process of each powder and the corresponding CO₂ emissions. These analyses are crucial for assessing the sustainability and environmental impact of the cementitious materials employed. The energy required to grind the various powders (clinker, gypsum, LF, and slag) was calculated based on Bond's third theory of comminution[60]. According to Bond's law, the energy consumption for grinding is proportional to the new surface area generated, which can be expressed as:

$$E = 10 * W_i \left(\frac{1}{\sqrt{P80}} - \frac{1}{\sqrt{F80}} \right) \quad (4)$$

Where; E is the energy consumption (kWh/ton); W_i is the Bond work index (kWh/ton); P80 is the 80% passing size of the product (μm); F80 is the 80% passing size of the feed (μm).

Using this equation, the energy consumption for grinding 1 ton of each powder was calculated basing on the SME Handbook for Mineral Processing [61]. Table 6 summarizes the energy consumption values for clinker, gypsum, LF, and slag. The energy consumption

values were converted to CO₂ emissions using the grid emissions factor specific to Algeria, which is 0.73 kgCO₂/kWh [62]. The CO₂ emissions for grinding each powder were calculated using the following formula:

$$\text{CO}_2 \text{ emissions (kg CO}_2\text{/ton)} = \text{Energy consumption (kWh/ton)} \times 0.73 \quad (5)$$

Table 5. Energy consumption and Carbone emission for grinding 1 ton

	Wi (kWh/ton)	P80 (μm)	F80 (μm)	E (kWh/ton)	CO ₂ emissions (kg/ton)
Clinker	13.6	32	5000	22.12	16.15
Gypsum	7.42	36	3000	11.01	8.04
Slag S1	13.4	14.6	3000	32.62	23.81
Slag S2	13.4	10.23	3000	39.45	28.80
LF L1	11.22	16.8	3000	25.33	18.49
LF L2	11.22	11.25	3000	31.40	22.92

Fig. 10 illustrates the CO₂ emissions and the embodied CO₂ parameters, which represents the ratio of CO₂ emissions to the compressive strength after one year, for various mixtures, providing a clear visual representation of their environmental efficiency. The results of the energy consumption and the Carbone emissions for grinding 1 ton of each powder are also illustrated in Table 5. The analysis reveals that the grinding process for each material results in different levels of energy consumption and CO₂ emissions. Slag and LF grinding is typically the most energy-intensive process, resulting in the highest CO₂ emissions. Conversely, clinker and gypsum require less energy to grind, resulting in lower CO₂ emissions. However, when considering the embodied CO₂ parameter, which represents the ratio of CO₂ emissions to the compressive strength of the mixtures after one year, a more nuanced picture emerges.

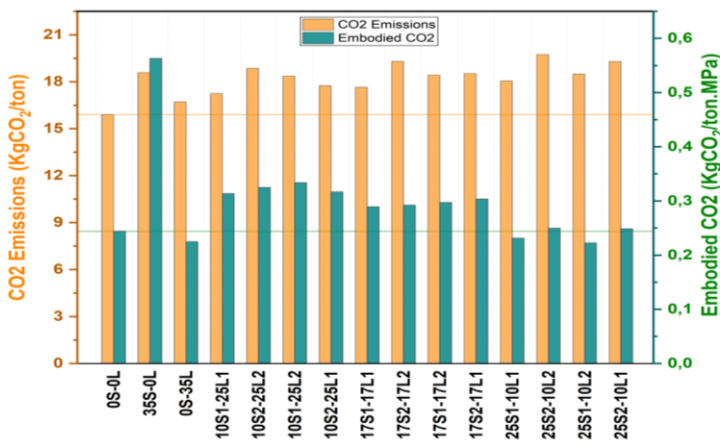


Fig. 10. CO₂ emissions and embodied CO₂ parameter results of each mixture

Mixtures such as 35S-0L exhibit the highest embodied CO₂ values due to the significant CO₂ emissions associated with high slag content and their low strength. On the other hand, mixtures incorporating higher proportions of LF and slag, such as 0S-35L and 25S1-10L2, demonstrate the lowest embodied CO₂ values. This indicates that substituting clinker with LF and slag not only reduces CO₂ emissions but also enhances environmental efficiency by

improving compressive strength relative to the carbon footprint. For instance, the mixture 25S1-10L2, with an embodied CO₂ value of 0.22 kgCO₂/ton.MPa, represents the best environmental efficiency among the tested mixtures, achieving a balance between lower emissions and robust structural performance.

4. Conclusion

This study assessed various mortars containing different proportions of limestone filler (LF) and blast furnace slag (BFS) powder, commonly used as cementitious materials. The findings yielded the following conclusions:

- Ternary mortars containing limestone filler (LF) and slag (BFS) exhibited significantly higher compressive strength compared to mortar with only 35% slag. After 7 days of curing, the ternary mortars showed a remarkable 62% increase in strength, and this improvement remained substantial at 31% after 28 days. Additionally, the compressive strength of ternary mortars was found to be 8.23-14% higher than that of OPC-0L-0S after 365 days.
- The fineness of materials significantly influenced the reaction of ternary mixtures (LF+BFS) in both short-term and long-term scenarios, particularly concerning limestone fillers.
- Adequate amounts of alumina sources (BFS) were necessary in ternary mixtures to ensure the formation of carboaluminates for up to 3 years.
- There were consistent variations in flexural and compressive strength, with a perfect linear relationship ($R^2 = 0.97$) observed through correlation analysis.
- Ternary mixtures exhibited a dense, compact, and less porous microstructure, as evidenced by SEM and mercury porosity tests, attributed to the presence of C-A-S-H and carboaluminate.
- The inclusion of LF with BFS in cementitious composites (17S1-17L1) improved resistance to CO₂ diffusion by 80% compared to mixtures with only 35% BFS, resulting in a permeability decrease of over 100% at 28 days for 17S1-17L1 compared to 35S-0L. These findings were consistent with mercury porosimeter tests.
- The cement mixture containing 35% slag exhibited a significant decrease in compressive strength after 200 days in 1.5% hydrochloric acid compared to all other mixtures. However, all ternary mixtures demonstrated substantial improvement in acid resistance, ranging from 45-80%.
- The optimal mix in terms of mechanical performance and durability was found to be 25S1-10L, with an optimal LF content of 10%.

In conclusion, the development of eco-efficient materials with high performance and reduced cement content (substituted with a combination of slag and limestone filler) did not compromise long-term strength and durability against carbonation and hydrochloric acid attack. On the contrary, depending on the added fines, it significantly enhanced durability performance, ensuring longer-lasting constructions made with concrete containing such mortar formulations.

Acknowledgments

The authors express their sincere gratitude to the laboratory staff at the University of Bordj Bou Arreridj and the C-MADE Covilhã laboratory at UBI University for their support.

References

- [1] Soldado E, Antunes A, Costa H, et al. Durability of mortar matrices of low-cement concrete with specific additions. *Construction and Building Materials*. 2021;309:125060. <https://doi.org/10.1016/j.conbuildmat.2021.125060>
- [2] Mahasenan N, Smith S, Humphreys K, editors. The cement industry and global climate change: current and potential future cement industry CO2 emissions. *Greenhouse gas control technologies-6th international conference*; 2003: Elsevier. <https://doi.org/10.1016/B978-008044276-1/50157-4>
- [3] Fennis SA, Walraven JC, Den Uijl JA. The use of particle packing models to design ecological concrete. *Heron*. 2009;54(2/3).
- [4] Schneider M, Romer M, Tschudin M, et al. Celitement: a sustainable prospect for the cement industry. *Cem Concr Res*. 2011;41:642-650. <https://doi.org/10.1016/j.cemconres.2011.03.019>
- [5] Sadok AH, Courard L. Chloride diffusion and oxygen permeability of mortars with low active blast furnace slag. *Construction and Building Materials*. 2018;181:319-324. <https://doi.org/10.1016/j.conbuildmat.2018.06.036>
- [6] Chidiac S, Panesar D. Evolution of mechanical properties of concrete containing ground granulated blast furnace slag and effects on the scaling resistance test at 28 days. *Cement and Concrete Composites*. 2008;30(2):63-71. <https://doi.org/10.1016/j.cemconcomp.2007.09.003>
- [7] Hadj Sadok R, Maherzi W, Benzerzour M, et al. Mechanical properties and microstructure of low carbon binders manufactured from calcined canal sediments and ground granulated blast furnace slag (GGBS). *Sustainability*. 2021;13(16):9057. <https://doi.org/10.3390/su13169057>
- [8] Deboucha W, Sebaibi N, El Mendili Y, et al. Reactivity effect of calcium carbonate on the formation of carboaluminate phases in ground granulated blast furnace slag blended cements. *Sustainability*. 2021;13(11):6504. <https://doi.org/10.3390/su13116504>
- [9] Deboucha W, Leklou N, Khelidj A. Combination effect of limestone filler and slag on hydration reactions in ternary cements. *European Journal of Environmental and Civil Engineering*. 2022;26(9):3931-3946. <https://doi.org/10.1080/19648189.2020.1825233>
- [10] Najm O, El-Hassan H, El-Dieb A. Ladle slag characteristics and use in mortar and concrete: A comprehensive review. *Journal of Cleaner Production*. 2021;288:125584. <https://doi.org/10.1016/j.jclepro.2020.125584>
- [11] Salvador RP, Rambo DA, Bueno RM, et al. On the use of blast-furnace slag in sprayed concrete applications. *Construction and Building Materials*. 2019;218:543-555. <https://doi.org/10.1016/j.conbuildmat.2019.05.132>
- [12] Bougara A, Lynsdale C, Ezziane K. Activation of Algerian slag in mortars. *Construction and Building Materials*. 2009;23(1):542-547. <https://doi.org/10.1016/j.conbuildmat.2007.10.012>
- [13] Kumar S, Kumar R, Bandopadhyay A, et al. Mechanical activation of granulated blast furnace slag and its effect on the properties and structure of portland slag cement. *Cement and Concrete Composites*. 2008;30(8):679-685. <https://doi.org/10.1016/j.cemconcomp.2008.05.005>
- [14] Bouasker M, Khalifa NEH, Mounanga P, et al. Early-age deformation and autogenous cracking risk of slag-limestone filler-cement blended binders. *Construction and Building Materials*. 2014;55:158-167. <https://doi.org/10.1016/j.conbuildmat.2014.01.037>
- [15] Celik K, Hay R, Hargis CW, et al. Effect of volcanic ash pozzolan or limestone replacement on hydration of Portland cement. *Construction and Building Materials*. 2019;197:803-812. <https://doi.org/10.1016/j.conbuildmat.2018.11.193>

- [16] Dhandapani Y, Santhanam M. Investigation on the microstructure-related characteristics to elucidate performance of composite cement with limestone-calcined clay combination. *Cement and Concrete Research*. 2020;129:105959. <https://doi.org/10.1016/j.cemconres.2019.105959>
- [17] Adu-Amankwah S, Zajac M, Stabler C, et al. Influence of limestone on the hydration of ternary slag cements. *Cement and Concrete Research*. 2017;100:96-109. <https://doi.org/10.1016/j.cemconres.2017.05.013>
- [18] Bullard JW, Jennings HM, Livingston RA, et al. Mechanisms of cement hydration. *Cement and Concrete Research*. 2011;41(12):1208-1223. <https://doi.org/10.1016/j.cemconres.2010.09.011>
- [19] Berodier E, Scrivener K. Understanding the Filler Effect on the Nucleation and Growth of C-S-H. *Journal of the American Ceramic Society*. 2014;97(12):3764-3773. <https://doi.org/10.1111/jace.13177>
- [20] De Weerdt K, Kjellsen K, Sellevold E, et al. Synergy between fly ash and limestone powder in ternary cements. *Cement and Concrete Composites*. 2011;33(1):30-38. <https://doi.org/10.1016/j.cemconcomp.2010.09.006>
- [21] Vickers NJ. Animal communication: when I'm calling you, will you answer too? *Current Biology*. 2017;27(14). <https://doi.org/10.1016/j.cub.2017.05.064>
- [22] Antoni M, Rossen J. Cement Substitution by a Combination of Metakaolin and Limestone. *Cement and Concrete Research*. 2012;42(12):1579-1589. <https://doi.org/10.1016/j.cemconres.2012.09.006>
- [23] Adu-Amankwah S, Black L, Skocek J, et al. Effect of sulfate additions on hydration and performance of ternary slag-limestone composite cements. *Construction and Building Materials*. 2018;164:451-462. <https://doi.org/10.1016/j.conbuildmat.2017.12.165>
- [24] Matschei T, Lothenbach B, Glasser F. The AFm phase in Portland cement. *Cement and Concrete Research*. 2007;37(2):118-130. <https://doi.org/10.1016/j.cemconres.2006.10.010>
- [25] Gao T, Dai T, Shen L, et al. Benefits of using steel slag in cement clinker production for environmental conservation and economic revenue generation. *Journal of Cleaner Production*. 2021;282:124538. <https://doi.org/10.1016/j.jclepro.2020.124538>
- [26] Carrasco-Maldonado F, Spörl R, Fleiger K, et al. Oxy-fuel combustion technology for cement production-state of the art research and technology development. *International Journal of Greenhouse Gas Control*. 2016;45:189-199. <https://doi.org/10.1016/j.ijggc.2015.12.014>
- [27] Menéndez G, Bonavetti V, Irassar E. Strength development of ternary blended cement with limestone filler and blast-furnace slag. *Cement and Concrete Composites*. 2003;25(1):61-67. [https://doi.org/10.1016/S0958-9465\(01\)00056-7](https://doi.org/10.1016/S0958-9465(01)00056-7)
- [28] Yu L, Wang Q, Wu K, et al. Identification of multi-scale homogeneity of blended cement concrete: Macro performance, micro and meso structure. *Journal of Thermal Analysis and Calorimetry*. 2022:1-12.
- [29] Xuan M-Y, Han Y, Wang X-Y. The hydration, mechanical, autogenous shrinkage, durability, and sustainability properties of cement-limestone-slag ternary composites. *Sustainability*. 2021;13(4):1881. <https://doi.org/10.3390/su13041881>
- [30] Arora A, Sant G, Neithalath N. Ternary blends containing slag and interground/blended limestone: Hydration, strength, and pore structure. *Construction and Building Materials*. 2016;102:113-124. <https://doi.org/10.1016/j.conbuildmat.2015.10.179>
- [31] Itim A, Ezziane K, Kadri E-H. Compressive strength and shrinkage of mortar containing various amounts of mineral additions. *Construction and Building Materials*. 2011;25(8):3603-3609. <https://doi.org/10.1016/j.conbuildmat.2011.03.055>
- [32] Briki Y, Zajac M, Haha MB, et al. Impact of limestone fineness on cement hydration at early age. *Cement and Concrete Research*. 2021;147:106515. <https://doi.org/10.1016/j.cemconres.2021.106515>

- [33] EN-196-1. Methods of testing cement-Part 1: Determination of strength. Quality and Standards Authority of Ethiopia, ES. 2005:1176-1.
- [34] Ibáñez-Gosálvez J, Real-Herraiz T, Ortega JM. Microstructure, durability and mechanical properties of mortars prepared using ternary binders with addition of slag, fly ash and limestone. Applied Sciences. 2021;11(14):6388. <https://doi.org/10.3390/app11146388>
- [35] Horpibulsuk S, Rachan R, Chinkulkijniwat A, et al. Analysis of strength development in cement-stabilized silty clay from microstructural considerations. Construction and Building Materials. 2010;24(10):2011-2021. <https://doi.org/10.1016/j.conbuildmat.2010.03.011>
- [36] Klinkenberg L. The permeability of porous media to liquids and gases. Am Petrol Inst, Drilling and Production Practice. 1941;2:200-213.
- [37] Perraton D. La perméabilité aux gaz des bétons hydrauliques. Toulouse; 1992.
- [38] Rozière E. Etude de la durabilité des bétons par une approche performantielle. Nantes; 2007.
- [39] P18-458 X. Tests for Hardened Concrete-Accelerated Carbonation Test-Measurement of the Thickness of Carbonated Concrete. AFNOR: Paris, France; 2008.
- [40] Benkaddour M, Aoual FK, Semcha A. Durabilité des mortiers à base de pouzzolane naturelle et de pouzzolane artificielle. Nature & Technology. 2009;(1):63.
- [41] Dubois V, Abriak NE, Zentar R, et al. The use of marine sediments as a pavement base material. Waste Management. 2009;29(2):774-782. <https://doi.org/10.1016/j.wasman.2008.05.004>
- [42] Dhandapani Y, Santhanam M, Kaladharan G, et al. Towards ternary binders involving limestone additions-A review. Cement and Concrete Research. 2021;143:106396. <https://doi.org/10.1016/j.cemconres.2021.106396>
- [43] Ballim Y, Graham PC. The effects of supplementary cementing materials in modifying the heat of hydration of concrete. Materials and Structures. 2009;42(6):803-811. <https://doi.org/10.1617/s11527-008-9425-3>
- [44] Avet F, Scrivener K. Investigation of the calcined kaolinite content on the hydration of Limestone Calcined Clay Cement (LC3). Cement and Concrete Research. 2018;107:124-135. <https://doi.org/10.1016/j.cemconres.2018.02.016>
- [45] Federico L, Chidiac S. Waste glass as a supplementary cementitious material in concrete-critical review of treatment methods. Cement and Concrete Composites. 2009;31(8):606-610. <https://doi.org/10.1016/j.cemconcomp.2009.02.001>
- [46] Aoual-Benslafa FK, Kerdal D, Ameur M, et al. Durability of mortars made with dredged sediments. Procedia Engineering. 2015;118:240-250. <https://doi.org/10.1016/j.proeng.2015.08.423>
- [47] Manmohan D, Mehta P. Influence of pozzolanic, slag, and chemical admixtures on pore size distribution and permeability of hardened cement pastes. Cement, Concrete and Aggregates. 1981;3(1):63-67. <https://doi.org/10.1520/CCA102031>
- [48] Hadj-sadok A, Kenai S, Courard L, et al. Microstructure and durability of mortars modified with medium active blast furnace slag. Construction and Building Materials. 2011;25(2):1018-1025. <https://doi.org/10.1016/j.conbuildmat.2010.06.077>
- [49] Tsivilis S, Tsantilas J, Kakali G, et al. The permeability of Portland limestone cement concrete. Cement and Concrete Research. 2003;33(9):1465-1471. [https://doi.org/10.1016/S0008-8846\(03\)00092-9](https://doi.org/10.1016/S0008-8846(03)00092-9)
- [50] Panesar DK, Zhang R. Performance comparison of cement replacing materials in concrete: Limestone fillers and supplementary cementing materials-A review. Construction and Building Materials. 2020;251:118866. <https://doi.org/10.1016/j.conbuildmat.2020.118866>
- [51] Carrasco M, Menéndez G, Bonavetti V, et al. Strength optimization of "tailor-made cement" with limestone filler and blast furnace slag. Cement and Concrete Research. 2005;35(7):1324-1331. <https://doi.org/10.1016/j.cemconres.2004.09.023>

- [52] Gruyaert E, Van den Heede P, De Belie N. Carbonation of slag concrete: Effect of the cement replacement level and curing on the carbonation coefficient-Effect of carbonation on the pore structure. *Cement and Concrete Composites*. 2013;35(1):39-48. <https://doi.org/10.1016/j.cemconcomp.2012.08.024>
- [53] L'Hôpital E, Lothenbach B, Le Saout G, et al. Incorporation of aluminium in calcium-silicate-hydrates. *Cement and Concrete Research*. 2015;75:91-103. <https://doi.org/10.1016/j.cemconres.2015.04.007>
- [54] Matschei T, Lothenbach B. Thermodynamic properties of Portland cement hydrates in the system CaO-Al₂O₃-SiO₂-CaSO₄-CaCO₃-H₂O. *Cement and Concrete Research*. 2007;37(10). <https://doi.org/10.1016/j.cemconres.2007.06.002>
- [55] Khalifa NEH, Bouasker M, Mounanga P, et al. Physicochemical study of cementitious materials based on binary and ternary binders. *Chemistry and Materials Research*. 2013;4:24.
- [56] Santhanam M, Cohen MD, Olek J. Effects of gypsum formation on the performance of cement mortars during external sulfate attack. *Cement and Concrete Research*. 2003;33(3):325-332. [https://doi.org/10.1016/S0008-8846\(02\)00955-9](https://doi.org/10.1016/S0008-8846(02)00955-9)
- [57] Makhoulfi Z, Kadri E, Bouhicha M, et al. Resistance of limestone mortars with quaternary binders to sulfuric acid solution. *Construction and Building Materials*. 2012;26(1):497-504. <https://doi.org/10.1016/j.conbuildmat.2011.06.050>
- [58] Boubekour T, Boulekbache B, Aoudjane K, et al. Prediction of the durability performance of ternary cement containing limestone powder and ground granulated blast furnace slag. *Construction and Building Materials*. 2019;209:215-221. <https://doi.org/10.1016/j.conbuildmat.2019.03.120>
- [59] Siad H, Lachemi M, Sahmaran M, et al. Effect of glass powder on sulfuric acid resistance of cementitious materials. *Construction and Building Materials*. 2016;113:163-173. <https://doi.org/10.1016/j.conbuildmat.2016.03.049>
- [60] Bond FC. Crushing and grinding calculations, Part I. *Br Chem Eng*. 1961;6:378-385.
- [61] Weiss NL. *SME mineral processing handbook*. New York: Society of Mining Engineers; 1985.
- [62] Belkadi AA, Kessal O, Berkouche A, et al. Experimental investigation into the potential of recycled concrete and waste glass powders for improving the sustainability and performance of cement mortars properties. *Sustainable Energy Technologies and Assessments*. 2024;64:103710. <https://doi.org/10.1016/j.seta.2024.103710>